Eur. Phys. J. D **37**, 23–28 (2006)
DOI: 10.1140/epjd/e2005-00261-y

THE EUROPEAN PHYSICAL JOURNAL D

Measurement of the photoionization cross-section of the $3p\,^2P_{1/2,3/2}$ excited levels of sodium

N. Amin, S. Mahmood, M. Anwar-ul-Haq, M. Riaz, and M.A. Baig[a]

Atomic and Molecular Physics Laboratory, Department of Physics, Quaid-i-Azam University, Islamabad 45320, Pakistan

Received 6 January 2005 / Received in final form 18 May 2005
Published online 27 September 2005

Abstract. The photoionization cross-section and number density of the $3p\,^2P_{1/2,3/2}$ excited levels of sodium have been measured as a function of the laser energy using two-step laser excitation in conjunction with a thermionic diode working in the space charge limited mode. Employing the saturation technique, the cross-sections for the $3p\,^2P_{1/2}$ and $3p\,^2P_{3/2}$ levels are determined as 2.16 (43) Mb and 3.74 (74) Mb respectively.

PACS. 32.30.Jc Visible and ultraviolet spectra – 32.80.Rm Multiphoton ionization and excitation to highly excited states (e.g., Rydberg states)

1 Introduction

The photoionization cross-sections of atoms from the ground state are well-known for many atoms [1,2] but comparatively little information is available about the cross-sections from the excited states. Laser spectroscopic techniques have augmented studies of multi-step and multi-photon photoionization processes. The higher intensity, narrow bandwidth and tunable radiation of dye lasers play a vital role for the selective excitation of any atomic level, and subsequent photoionization from a given excited state to measure the cross-section of the pertinent state. Rothe et al. [3,4] pioneered the photoionization cross-section for the excited states of Na and Li based on studies of the radiative electron-ion recombination and shock-heated plasma. Ambartzumian et al. [5] pioneered the work on the measurement of the photoionization cross-section using the saturation technique and measured the photoionization cross-section of the $6p\,^2P_{1/2}$ and $^2P_{3/2}$ levels of rubidium. This technique was extended by Heinzmann et al. [6] to measure the photoionization cross-section of the $7p\,^2P_{1/2}$ and $^2P_{3/2}$ levels of cesium. Duong et al. [7] discussed the importance of atomic alignment and the light polarization and measured the relative cross-section of the sodium $3p$ level. Subsequently, Smith et al. [8] measured the absolute cross-section for the photoionization of the $4d$ and $5s$ excited states of sodium using 1.064 μm laser radiation. Effects of polarization in the measurement of the cross-section were also investigated. Garver et al. [9] reported the atomic densities of the $3p\,^2P_{1/2,3/2}$ levels of sodium by using the radiation-trapping technique. They also measured the apparent life times of the $3p\,^2P_{1/2}$ and $^2P_{3/2}$ levels as a function of atomic density. Preses et al. [10] reported the photoionization of the $3p$ excited state of sodium using a laser to populate the initial state and broad band synchrotron radiation for the ionizing process. Saha et al. [11] calculated the photoionization cross-section for the $4d$ excited state of sodium employing the multi-configuration Hartree-Fock method. Their results are in good agreement with the experimental results of Smith et al. [8], which were performed at single photon ionization. Burkhardt et al. [12] simultaneously determined the magnitude of the photoionization cross-section and the atomic density for the $3p\,^2P_{3/2}$ level of sodium. They used one laser beam to excite the atoms to the resonance level and a second laser beam for the ionization. The ionizing laser beam was focused to a diameter much smaller than that of the exciting laser by a lens. Beterov and Ryabtsev [13] reported the single and two-photon ionization of the $4s$-level of sodium. The experimental two-photon ionization cross-section of the $4s$ level at 1064 nm was obtained as $\sigma^{exp} = 5.6 \pm 2.9 \times 10^{-47}$ cm^4 s. The theoretical cross-section for the $4s$ state was also calculated within the framework of the three level model. Beterov et al. [14] reported the photoionization of the excited sodium atoms of the $4d$ state in the field of a train of ultra short pulses of a Nd:YAG laser. Kupliauskiene [15] calculated the single and shake up photoionization cross-section of sodium atom in the ground and first excited states using the relaxed-orbital MCH approach. Petrov et al. [16] reported the partial and total photoionization of the excited alkali atoms (Na, K, Rb and Cs) using configuration interaction technique with Pauli-Fock orbitals (CIPF). They also discussed the effect of the polarization of the atomic core with the valence electron. The relative photoionization cross-section of potassium ($4p\,^2P_{3/2}$) over the photoelectron energy range 0–0.22 eV for parallel and

[a] e-mail: baig@qau.edu.pk

perpendicular linear polarizations of the two laser beams was also reported. Petrov et al. [16] also reported the absolute values of the cross-section determined at three selected photoelectron energies. Vsevolodskii and Chernenko [17] reported the photoionization cross-section of the excited sodium atoms of the $4d$ state in the field of nanoseconds pulses of a Nd:YAG laser.

Magneto optical trap (MOT) has also been successfully used for measuring the absolute photoionization cross-sections of excited alkali atoms. This technique was first introduced by Dinneen et al. [18], who pioneered the MOT loaded by an atomic beam to measure the photoionization cross-section of the $5p\,^2\mathrm{P}_{3/2}$ level in atomic rubidium. Subsequently, similar technique was used to measure the photoionization cross-sections for rubidium [19], cesium [20,22] and for sodium and lithium [25]. Marago et al. [20] reported the absolute photoionization cross-section of laser-cooled cesium atoms in the first excited state $6p\,^2\mathrm{P}_{3/2}$ at various wavelengths while Patterson et al. [22] reported the absolute photoionization cross-section of the same level (Cs $6p\,^2\mathrm{P}_{3/2}$) by monitoring the decay of trap fluorescence during exposure to the ionizing laser radiation. Gabbanini et al. [21] reported the relative measurements of the partial photoionization cross-sections of the trapped rubidium atoms. Arimondo et al. [24] also reported careful experiments on the laser-cooled alkali atoms by irradiating Rb and Cs MOT's with a photoionizing laser beam. They analyzed the loading behaviour of the traps to determine the photoionization cross-section of the excited states of these elements based on a trap load/loss model. Fuso et al. [23] reported the photoionization experiments on the laser cooled Cs and Rb atoms and discussed the role of processes like ion diffusion and recombination, determination of the time evolution and the rate of the produced atomic ions. Wippel et al. [25] reported the photoionization cross-section of the first excited states of sodium and lithium at different ionizing lasers using magneto-optical trap. The fraction of trapped atoms in the first excited state was ionized using the UV-laser radiation. With the help of the loading curve they evaluated the photoionization cross-sections of sodium at eight different wavelengths between 334 to 408 nm.

The present paper describes measurement of the photoionization cross-sections of the $3p\,^2\mathrm{P}_{1/2}$ and $^2\mathrm{P}_{3/2}$ levels of sodium and the determination of the number density by using the saturation technique. Our results for the photoionization cross-section and the number density for the $3p\,^2\mathrm{P}_{3/2}$ level are in good agreement with the known values, whereas the corresponding photoionization cross-section for the $3p\,^2\mathrm{P}_{1/2}$ level is reported for the first time.

2 Experimental set-up

The experimental arrangement to study the photoionization from the first excited states of sodium is similar as described in our earlier work [26] and is shown in Figure 1. We have used a Nd:YAG laser system (Spectra, GCR-11), operated in the Q-Switched mode, for pumping a locally made Hanna type [27] dye laser. Sodium vapor was produced in a thermionic diode composed of a stainless steel tube 48 cm long, 3 cm in diameter and 1 mm wall thickness. About 20 cm of the central part of the tube was heated by a clamp-shell oven operating at a temperature 640 K that corresponds to about ≈0.2 Torr vapor pressure of sodium. Argon gas at a pressure of ≈0.5 Torr was used as a buffer gas. The temperature was monitored by a Ni–Cr–Ni thermocouple and it was maintained with in ±1% by a temperature controller. A 0.2 mm thick tungsten wire, stretched axially along the tube was heated by a separate regulated power supply that served as cathode for the ion detection.

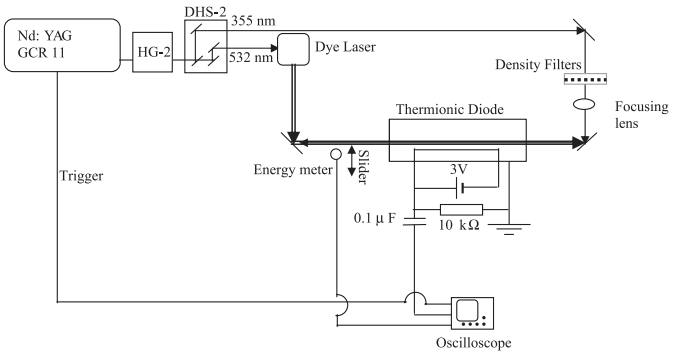

Fig. 1. A schematic diagram of the experimental set-up. A linearly polarized laser beam is used to populate the $3p\,^2\mathrm{P}_{1/2}$ and $^2\mathrm{P}_{3/2}$ levels. The THG (355 nm) of a Nd:YAG laser is used as an ionizing laser.

The experiments were performed using a two-step excitation technique. The first dye laser, charged with R590 dye dissolved in methanol and pumped by the SHG (532 nm) of the Nd:YAG laser was used to excite the atoms from the ground state to the $3p\,^2\mathrm{P}_{1/2}$ level lying at 589.6 nm in the first experiment and to the $3p\,^2\mathrm{P}_{3/2}$ level lying at 589.0 nm in the second experiment. The dye laser pulse energy was ≈1 mJ, band width ≤0.3 cm^{-1} and beam spot diameter ≈2 mm. The energy of the first (exciting) laser was adjusted such that the excitation signal from the $3p$ level can easily be saturated. The THG (355 nm) of the same Nd:YAG laser was used as an ionizing laser beam. The laser beam was focused to a diameter, much smaller than that of the exciting laser beam, by a long focal length lens. The diameter of the ionizing laser was 230–280 μm and its energy was measured by an energy meter. Both, exciting and ionizing laser beams were temporally overlapped. The intensity of the ionizing laser was varied using neutral density filters (Edmund). The ion signal was taken across a 10 kΩ resistor through a 0.01 μF blocking capacitor and was registered on a 100 MHz storage oscilloscope.

3 Results and discussions

The probability of a transition occurring from one state to another is directly proportional to the population of the state from which the transition takes place. When the lower state is more populated than the upper state,

the upward transitions predominate and absorption of energy occurs from the radiation beam. When the populations of both the levels become comparable, the upward and downward transitions reach equilibrium, and no further absorption takes place. At this moment the system is termed in the saturation state (Letokhov [28] and references therein). In the multi-step excitation/ionization process, atoms are excited to an intermediate level by the exciting laser and photoionization from that level is achieved by the second (ionizing) laser. The multi-step photoionization depends upon the flux of the ionizing laser pulse, which enables absolute measurement of the photoionization cross-section. Burkhardt et al. [12] applied the two-step ionization technique for the measurement of the absolute cross-section from the excited states and the atomic density for Na ($3p\,^2\mathrm{P}_{3/2}$), K ($4p\,^2\mathrm{P}_{3/2}$) and Ba ($6s6p\,^1\mathrm{P}_1$). These experiments were performed at a higher laser intensity of the excitation laser than required to saturate the resonance transition. Under such condition, the Rabi frequency is high enough that the spontaneous emission can be ignored during the 10 ns laser pulse. The total charge per pulse is represented by the relation:

$$Q = eN_0V_{vol}\left[1-\exp\left(-\frac{\sigma U}{2\hbar\omega A}\right)\right] \tag{1}$$

where e (coulomb) is the electronic charge, N_0 (cm^{-3}) is the density of the excited atoms, A (cm^2) is the cross-sectional area of the ionizing laser beam, U (Joule) is the total energy per ionizing laser pulse, $\hbar\omega$ (Joule) is the energy per photon of the ionizing laser beam, V_{vol} (cm^3) is the laser interaction volume and σ (cm^2) is the absolute cross-section for photoionization.

The number of ions per unit volume can be determined from the relation:

$$N = \frac{Q}{eV_{vol}}. \tag{2}$$

However, substituting the value of Q in this equation gives the following expression:

$$N = N_0\left[1-\exp\left(-\frac{\sigma U}{2\hbar\omega A}\right)\right]. \tag{3}$$

All the quantities in equation (3) are either known or measured except N_0 and σ, which can be determined by a least squares fit of the experimentally observed data.

From the ion signal the number of ions yield is calculated using the following relation:

$$N = \frac{Q}{eV_{vol}} = \frac{I(\mathrm{mA})\times t(\mathrm{s})}{e(\mathrm{coulomb})\times V_{vol}(\mathrm{cm}^3)}$$

$$\text{or,}\quad N = \frac{V(\mathrm{volts})\times t(\mathrm{s})}{R(\mathrm{ohms})\times e(\mathrm{coulombs})\times V_{vol}(\mathrm{cm}^3)} \tag{4}$$

where V is the signal height in volts, t is the temporal width in seconds at the optimum value of the signal, R is the input impedance of the detection system, e is the electronic charge and V_{vol} is the laser interaction volume.

He et al. [29] reported the absolute photoionization cross-section of the $6s6p\,^1\mathrm{P}_1$ excited state of barium. Their method for determining the photoionization cross-section is an extension of the saturation technique described by Burkhardt et al. [12]. They obtained their results by accounting the effects for the Gaussian laser intensity distribution. Mende et al. [30] acquired the photoionization cross-section by modifying equation (1) and presented

$$Z = \int_V N_0\left(1-\exp\left(-\frac{1}{2}\sigma^{1+}g\left(\rho\right)\phi\right)\right)dV. \tag{5}$$

Here Z is the total charge per pulse, N_0 is the number density of the excited level, σ^{1+} is the cross-section for photoionization, ϕ is the time-integrated number of photons of the ionizing laser pulse and $g\left(\rho\right)$ is the spatial distribution of the laser pulse. For a Gaussian laser intensity distribution this function is represented as:

$$g(\rho) = \frac{1}{\pi\Delta\rho^2}\exp\left\{-\left(\frac{\rho}{\Delta\rho}\right)^2\right\} \tag{6}$$

where $\Delta\rho$ is the half width of the distribution profile.

In the present experiment we acquired the photoionization cross-section by using equation (5) under the best alignment conditions for the Gaussian laser intensity distribution. The measurement of the atomic density using the saturation technique depends on the interaction volume, which is defined by the volume of the laser beams in the ion collection region. The interaction volume depends on the optical properties of the focusing lens and the geometry of the apparatus. In the present experiment, the ionizing laser beam at 355 nm was focused by a long focal length lens. By the combination of iris aperture and focusing lens we managed to achieve nearly uniform laser beam intensity.

A schematic energy level diagram of sodium along with the relevant excitation paths is shown in Figure 2. From the $3s\,^2\mathrm{S}_{1/2}$ ground state, the sodium atoms can be promoted either to $3p\,^2\mathrm{P}_{1/2}$ or $3p\,^2\mathrm{P}_{3/2}$ level using the dye laser at 589.6 nm or 589.0 nm respectively. As the first dye laser is pumped by the second harmonic (532 nm) of a Nd:YAG laser therefore the laser light is linearly polarized

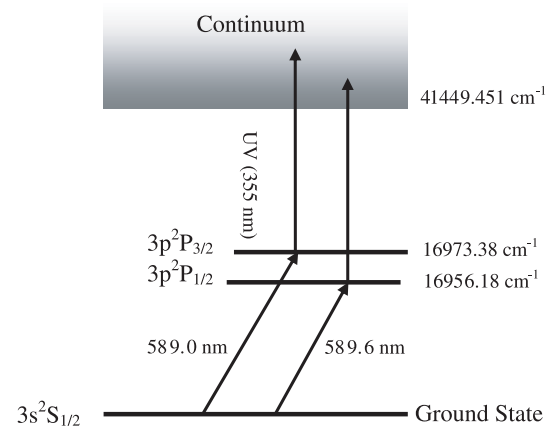

Fig. 2. Energy level diagram showing the two-step excitation and ionization paths.

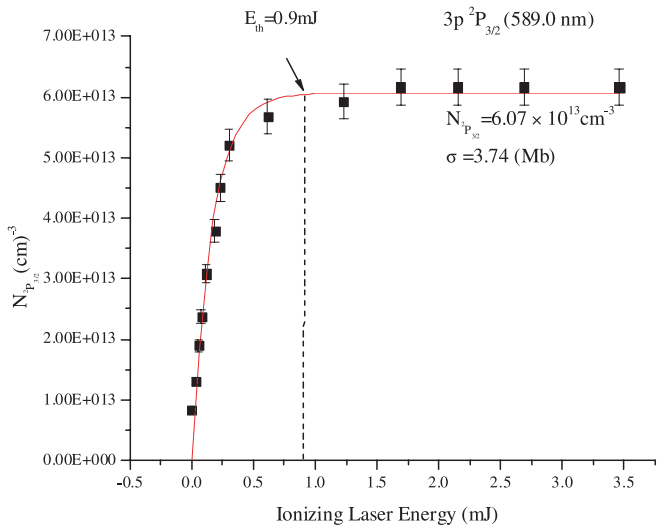

Fig. 3. The photoionization data for the (a) Na $(3p\,^2\mathrm{P}_{3/2})$ and the (b) Na $(3p\,^2\mathrm{P}_{1/2})$ levels. The solid line shown is the least square fit of equation (5) to the observed data for extracting the values of cross-section σ (Mb) and number density (cm^{-3}) for the resonance lines of sodium.

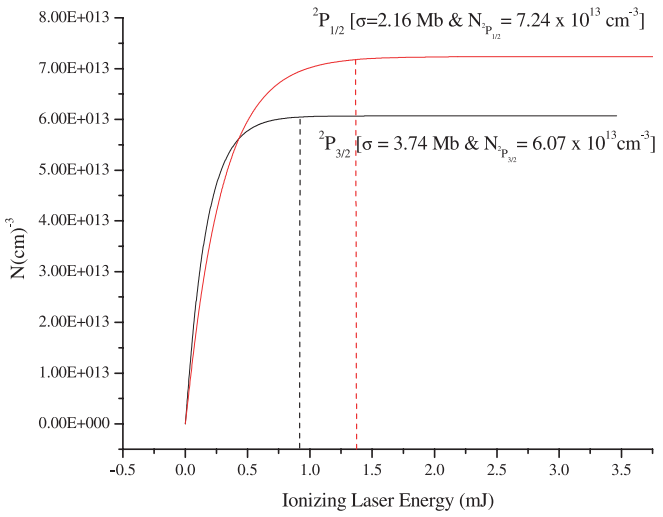

Fig. 4. A graph showing the comparison of the calculated data for the Na $(3p\,^2\mathrm{P}_{1/2})$ and $(3p\,^2\mathrm{P}_{3/2})$ levels using the extracted values of the cross-sections and number densities.

in the z-direction. Consequently, the assessable transition will follow $\Delta m_j = 0$ selection rules. The upper states will possess $m_j = +1/2$ and $-1/2$. In the second step the atoms from either the $^2\mathrm{P}_{1/2}$ or $^2\mathrm{P}_{3/2}$ level are ionized by the third harmonic (355 nm) of the Nd:YAG laser. The ionizing laser is also linearly polarized but its direction is horizontal with respect to the first step dye laser. The major contribution in the ionization comes from $\varepsilon s\,^2\mathrm{S}_{1/2}$ and $\varepsilon d\,^2\mathrm{D}_{3/2}$ channels based on polarization. Keeping the intensity of the exciting laser fixed and varying the intensity of the ionizing laser, using the neutral density filters, we have registered the ion signals. Typical data for the photoionization of the $3p\,^2\mathrm{P}_{1/2}$ and $3p\,^2\mathrm{P}_{3/2}$ levels are shown in Figures 3a and 3b. The circles including 5% error bars represent the experimental data points. The solid line, which passes through the data points, is a least squares fit using equation (5). It is evident from Figures 3a and 3b that as the laser intensity increases; the ion signal increases up to certain value and then the signal stops increasing further. At this point the photoionization from the first excited state reaches its maximum and saturation sets in. At saturation ionization the photon flux of the ionizing laser equalizes the population of the intermediates levels. The fitting of the experimental data for the $3p\,^2\mathrm{P}_{3/2}$ level yields the number density $N(^2\mathrm{P}_{3/2}) = 6.07\,(12)\times10^{13}$ cm^{-3} and the cross-section $\sigma = 3.74\,(74)$ Mb. The estimated uncertainty in the value of the photoionization cross-sections σ is $\pm$ 20%, which is due to the experimental errors in the measurements of the laser energy, diameter of the laser beam and calibration of the detection system. This value of cross-section is in good agreement with that reported by Burkhardt et al. [12] as 3.7(7) Mb. The photoionization cross-section extracted in the present work and that of Burkhardt et al. [12] were achieved using an 355 nm ionizing laser.

We extended our studies to the determination of the photoionization cross-section and number density for the $3p\,^2\mathrm{P}_{1/2}$ level. The data presented in Figure 3b yields $\sigma = 2.16\,(43)$ Mb and $N(^2\mathrm{P}_{1/2}) = 7.24\,(14)\times10^{13}$ cm^{-3} respectively. Since the aforementioned sub-level is explored for the first time therefore, a comparison of the photoionization cross-section is not possible. Rothe [3] reported the photoionization cross-section of the $3p$ levels as 7.63(90) Mb whereas, the calculated values of cross-section are 7.38 Mb Aymar et al. ([31] references are there in for other alkali metals) and 8.5 Mb Preses et al. [10].

The threshold laser energy E_{th} at which the saturation just sets in can be measured from the plots of the ionization signal against the ionizing laser energies (see Figs. 3 and 4). The measured values are 1.37 mJ and 0.9 mJ for the $3p\,^2\mathrm{P}_{1/2}$ and $3p\,^2\mathrm{P}_{3/2}$ levels respectively.

Table 1. Photoionization cross-sections of the resonance levels of alkali atoms.

Atom	Saturation method			MOT method			
	level	wavelength (nm)	cross-section (Mb) [Reference]	level	wavelength (nm)	cross-section (Mb) [Reference]	
Cs	$7p\,^2P_{1/2}$	459.3	6.2 ± 0.5 [6]	$6p\,^2P_{3/2}$	496.5	18.6 ± 1.5 [22]	
	$7p\,^2P_{3/2}$	455.5	8.8 ± 1.6 [6]			σ_p(Mb) from loss-rate data	σ_p(Mb) data for number of atoms
				$6p\,^2P_{3/2}$	497	17.2 ± 1.6 [20]	19.2 ± 1.7 [20]
					501	16.1 ± 1.6 [24]	18.6 ± 1.8 [24]
					497	17.2 ± 1.7 [24]	19.2 ± 1.9 [24]
					488	16.9 ± 1.7 [24]	15.8 ± 1.6[24]
					458	14.0 ± 1.4 [24]	14.1 ± 1.4 [24]
					422	11.5 ± 1.1 [24]	8.2 ± 0.8 [24]
Rb	$6p\,^2P_{1/2}$	694.3	15 ± 4 [5]	$5p\,^2P_{3/2}$	413	13.6 ± 1.2 [18]	
	$6p\,^2P_{3/2}$	694.3	17 ± 4 [5]	$5p\,^2P_{3/2}$	407	12.5 ± 1.1 [18]	
	$6p\,^2P_{3/2}$	347.1	19 ± 5 [5]	$5p\,^2P_{3/2}$	476.5	14.8 ± 2.2 [19]	
						$\sigma_{5p,cd}$(Mb)	$\sigma_{5p,cs}$(Mb)
				$5p\,^2P_{3/2}$	476	12.6 ± 2.5 [21]	2.2 ± 0.4 [21]
K	$4p\,^2P_{3/2}$	355	7.6 ± 1.1 [12]	$4p\,^2P_{3/2}$	—	—	
		351	7.0 ± 1 [16]				
Na	$3p\,^2P_{3/2}$	355	3.7 ± 0.7 [12]		351	1.2 ± 0.2 [25]	
					364	3.7 ± 0.7 [25]	
	$3p\,^2P_{1/2}$	355	2.16 ± 0.47 [present work]	$3p\,^2P_{3/2}$	399.5	8.4 ± 1.3 [25]	
					401.5	7.1 ± 1.1 [25]	
	$3p\,^2P_{3/2}$	355	3.74 ± 0.7 [present work]		404	9.1 ± 1.4[25]	
					407.8	6.9 ± 0.7 [25]	
^{7}Li	$2p$	350	19.7 ± 3 [4]	$2p$	334.47	16.2 ± 2.5 [25]	
					335.85	18.3 ± 2.8 [25]	

Burkhardt et al. [12] used an atomic beam of sodium that was crossed by the exciting and ionizing laser beams, resulting in a small interaction volume. Whereas, we have used a thermionic diode ion detector in which both the exciting and ionizing laser beams were spatially overlapped resulting a larger interaction volume. Mende and Kock [33,34] used an identical experimental set-up to measure the photoionization cross-section and oscillator strengths of the Rydberg series in strontium and barium. Kallenbach et al. [35] also used the thermionic diode for the measurement of photoionization cross-section of barium.

The measurements of atomic densities of the ground and excited states of sodium are well documented [9,12,32]. The reported values lie in the range 10^9 to 10^{13} cm^{-3}. A plausible reason for such variation might be the difference in the interaction volume due to the geometry of the apparatus and the collisional ionization rates. In our case the number density of the $3p\,^2P_{3/2}$ level is slightly lower than that of the $3p\,^2P_{1/2}$ level. This difference in the number densities may be attributed to the apparent difference in the lifetime of these levels. Although the natural lifetimes of the $^2P_{1/2}$ and $^2P_{3/2}$ are nearly the same ≈16 ns [36], but the apparent lifetime of each line is different due to their different absorption coefficients [9] that are known as 5×10^{11} cm^2 and 10×10^{11} cm^2 respectively [37].

In Table 1, we present values of absolute photoionization cross-sections of the excited levels of alkali atoms measured using the saturation and the MOT methods by different groups. Some selected values of the photoionization cross-section acquired by the MOT technique are also tabulated. From the data we can merely make any comparison between the two techniques because the levels studied for the Cs and Rb atoms are different. Nevertheless, for Na and Li the same excited levels were acquired employing different ionizing laser. It would be interesting to acquire the photoionization cross-sections of the excited alkali atoms at the same ionizing laser using these two techniques and to have a meaningful comparison. It is evident that the photoionization cross-section by using saturation technique is higher for $^2P_{3/2}$ than $^2P_{1/2}$ in Rb, Cs and Na (present work). The photoionization cross-section of $^2P_{1/2}$ of these elements so far has been not reported by using the MOT technique. The polarization effects could influence the results for the photoionization cross-section. The linearly polarized laser induces an alignment in the electron cloud of the intermediate level which influences the cross-section for the ionizing step in a way which depends on the angle between the electric vectors of the

two lasers and on the ratio of the relevant electric dipole matrix. Petrov et al. [16] also predicted that for parallel linearly polarized light the cross-section for Na($^2P_{3/2}$) level is expected to be higher than that for Na($^2P_{1/2}$). It will be interesting to extend these studies to lithium and potassium. In particular, the photoionization cross-section for the $4p\,^2P_{3/2}$in potassium is reported as 7.6 Mb [12] but to our knowledge it is still unknown for the $4p\,^2P_{1/2}$ level. We are planning to undertake this work in the near future.

The present work was financially supported by the Higher Education Commission (HEC), Pakistan Science Foundation (PSF-120), ICTP, Trieste, Italy under the ICAC affiliated centre scheme and the Quaid-i-Azam University, Islamabad, Pakistan. Nasir Amin is particularly grateful to the HEC for the grant of Ph.D. scholarship under the Indegenous scheme.

References

1. G.V. Marr, *Photoionization processes in gases* (Academic Press, New York, 1967)
2. J. Berkowitz, *Photoabsorption, Photoionization and Photoelectron Spectroscopy* (Academic Press, New York, 1979)
3. D.E. Rothe, J. Quant. Spectrosc. Radiat. Transfer **9**, 49 (1969)
4. D.E. Rothe, J. Quant. Spectrosc. Radiat. Transfer **11**, 355 (1971)
5. R.V. Ambartzumian, N.P. Furzikov, V.S. Letokhov, A.A. Puretsky, Appl. Phys. **9**, 335 (1976)
6. U. Heinzmann, D. Schinkowski, H.D. Zeman, Appl. Phys. **12**, 113 (1977)
7. H.T. Duong, J. Pinard, J.L. Vialle, J. Phys. B: At. Mol. Opt. Phys. **11**, 797 (1978)
8. A.V. Smith, J.E.M. Goldsmith, D.E. Nitz, S.J. Smith, Phys. Rev. A **22**, 577 (1980)
9. W.P. Garver, M.R. Pierce, J.J. Leventhal, J. Chem. Phys. **77**, 1201 (1982)
10. J.M. Preses, C.E. Burkhardt, R.L. Corey, D.L. Earsom, T.L. Daulton, W.P. Garver, J.J. Leventhal, A.Z. Msezane, S.T. Manson, Phys. Rev. A **32**, 1264 (1985)
11. H.P. Saha, M.S. Pindzola, R.N. Compton, Phys. Rev. A **38**, 128 (1988)
12. C.E. Burkhardt, J.L. Libbert, Jian Xu, J.J. Leventhal, J.D. Kelley, Phys. Rev. A **38**, 5949 (1988)
13. I.M. Beterov, I.I. Ryabtsev, Opt. Spectrosc. **75**, 313 (1993)
14. I.M. Beterov, I.I. Ryabtsev, E.V. Pestryakov, V.V. Petrov, V.I. Trunov, N.V. Fateev, A.A. Chernenko, Opt. Spectrosc. **81**, 383 (1996)
15. A. Kupliauskiene, J. Phys. B: At. Mol. Opt. Phys. **30**, 1865 (1997)
16. I.D. Petrov, V.L. Sukhorukov, E. Leber, H. Hotop, Eur. Phys. J. D **10**, 53 (2000)
17. E.V. Vsevolodskii, A.A. Chernenko, Opt. Spectrosc. **91**, 675 (2001)
18. T.P. Dinneen, C.D. Wallace, K.-Y. N. Tan, P.L. Gould, Opt. Lett. **17**, 1706 (1992)
19. C. Gabbanini, S. Gozzini, A. Lucchesini, Opt. Commun. **141**, 25 (1997)
20. O. Marago, D. Ciampini, F. Fuso, E. Arimondo, C. Gabbanini, S.T. Manson, Phys. Rev. A **57**, R4110 (1998)
21. C. Gabbanini, F. Ceccherini, S. Gozzini, A. Lucchesini, J. Phys. B: At. Mol. Opt. Phys. **31**, 4143 (1998)
22. B.M. Patterson, T. Takekoshi, R.J. Knize Phys. Rev. A **59**, 2508 (1999)
23. F. Fuso, D. Ciampini, E. Arimondo, C. Gabbanini, Opt. Commun. **173**, 223 (2000)
24. E. Arimondo, D. Ciampini, F. Fuso, C. Gabbanini, Appl. Surf. Sci. **154-155**, 527 (2000)
25. V. Wippel, C. Binder, W. Huber, L. Windholz, M. Allegrini, F. Fuso, E. Arimondo, Eur. Phys. J. D **17**, 285 (2001)
26. M.A. Baig, M. Akram, N.K. Piracha, M.S. Mahmood, S.A. Bhatti, N. Ahmad, J. Phys. B: At. Mol. Opt. Phys. **28**, 1421 (1995)
27. D. Hanna, P.A. Karkainen, R. Wyatt, Opt. Quant. Electron **7**, 115 (1975)
28. V.S. Letokhov, *Laser Photoionization Spectroscopy* (Academic Press, Orlando, FL, 1987)
29. L.W. He, C.E. Burkhardt, M. Ciocca, J.J. Leventhal, Phys. Rev. Lett. **67**, 2131 (1991)
30. W. Mende, K. Bartschat, M. Kock, J. Phys. B: At. Mol. Opt. Phys. **28**, 2385 (1995)
31. M. Aymar, E. Luc-Koenig, F.C. Farnoux, J. Phys. B: At. Mol. Opt. Phys. **9**, 1279 (1976)
32. T. Oomori, K. Ono, Y. Murai, J. Appl. Phys. **64**, 1619 (1988)
33. W. Mende, M. Kock, J. Phys. B: At. Mol. Opt. Phys. **29**, 655 (1996)
34. W. Mende, M. Kock, J. Phys. B: At. Mol. Opt. Phys. **30**, 5401 (1997)
35. A. Kallenbach, M. Kock, G. Zierer, Phy. Rev. A **38**, 2356 (1988)
36. W.L. Wiese, M.W. Smith, B.M. Miles, *Atomic Transition Probabilities*, Natl. Stand. Ref. Data Ser. Natl. Bur. Stand. (U.S. GPO, Washington D.C., 1969)
37. A.C.G. Mitchell, N.W. Zemansky, *Resonance Radiation and Excited Atoms* (Cambridge University, New York, 1934)
38. T. Arisawa, Y. Maruyama, Y. Suzuki, K Shiba, Appl. Phys. B **28**, 73 (1982)